Eur. Phys. J. A **4**, 195–203 (1999)

THE EUROPEAN PHYSICAL JOURNAL A

Deconfinement transition: a three dimensional model

W.M. Alberico[1], P. Czerski[2], M. Nardi[3]

[1] Dipartimento di Fisica Teorica dell'Università di Torino and INFN, Sezione di Torino via P.Giuria 1, 10125 Torino, Italy
[2] Instytut Fizyki Jądrowej Kraków, Poland
[3] Fakultät für Physik, Universität Bielefeld, D-33501 Bielefeld, Germany

Received: 10 June 1998 / Revised version: 24 September 1998
Communicated by F. Lenz

Abstract. We present a three–dimensional model for quark matter with a density dependent quark–quark (confining) potential, which allows to describe a sort of deconfinement transition as the system evolves from a low density assembly of bound structures to a high density free Fermi gas of quarks. We consider different confining potentials, some of which successfully utilized in hadron spectroscopy. We find that a proper treatment of the many–body correlations induced by the medium is essential to disentangle the different nature of the two (hadronic and deconfined) phases of the system. For this purpose the ground state energy per particle and the pair correlation function are investigated.

PACS. 24.85.+p Quarks, gluons, and QCD in nuclei and nuclear processes – 12.39.-x Phenomenological quark models – 12.39.Jh Nonrelativistic quark model – 12.38.Mh Quark-gluon plasma – 25.75.-q Relativistic heavy-ion collisions

1 Introduction

During the past decade a considerable effort has been carried out in experiments of nucleus–nucleus collisions at relativistic energies, looking for signals of colour deconfinement. In this situation the highly compressed hadronic matter of the colliding nuclei should undergo a peculiar phase transition into the so–called quark–gluon plasma (QGP), a state of matter possibly occurring in the early stages of the Universe.

The recent experimental evidence of an anomalous J/Ψ suppression in the analysis of the NA50 collaboration [1] lends itself to support the belief that deconfinement has been achieved at some stage of the collision, since the disappearance of J/Ψ in the final yield was long ago predicted [2] as a possible signature for QGP.

While theoretical analysis of these data are being carefully carried out [3], a microscopic description of the complex many–body dynamics which eventually underlies this phase transition is urged. As it is well known, the intrinsic nature of the QCD lagrangian and the non–perturbative character of the confined regime prevent its direct use within standard many–body frameworks.

Several phenomenological models have been thus proposed in the past, usually tailored to reproduce the known properties of quarks when confined into hadrons. As far as hadronic matter is concerned, the subnucleonic degrees of freedom are rarely felt to be worth introducing, especially for low energy nuclear properties. However, in relativistic heavy ion experiments, very high densities and temperatures of the colliding nuclei are potentially reached and quark degrees of freedom become dominant.

Non–relativistic constituent quark models for quark/nuclear matter have been proposed since many years [4–7] and have proven remarkably useful for single hadrons spectroscopy [8,9], in spite of the lack of Lorentz invariance and chiral symmetry. The finite mass of the constituent quarks is often assumed to be the result of the non–perturbative confining process inside hadrons.

The present work extends to the three–dimensional situation a non–relativistic "string–flip like" model, already successfully employed in one dimension to show up a hadron–quark gas transition when the density of the system increases [10]. An extension to finite temperatures has been also investigated (in a one–dimensional system) with sound results [11]. Beyond some naive confining forces, like a quadratic or a linear potential, we also employ the so–called Cornell potential, more realistically used for hadron spectroscopy.

We are mainly focussed on the many–body effects played by a dense medium on the quark–quark dynamics and thus we found it more appropriate to stick to a non–relativistic model. Indeed, in the literature, relativistic many–body approaches mainly rely on the mean–field approximation, while our work is centered on the in–medium two–body correlations. Admittedly, at very large densities, the non-relativistic treatment does not seem to be adequate: the simplest relativistic effect is kinematics and we shall discuss this point within a "minimal" prescription to account for it, while other effects like non–static terms in the potential (typically spin–dependent components of the two–body interaction) go beyond the scope of the present work.

The key ingredient of our model is a density dependent screening of the confining interaction between quarks: as it is well known in nuclear dynamics, density dependent forces mimic the effects of many–body interactions, which are expected to occur in a dense system of quarks. We assume therefore the following quark–quark potential:

$$V(\rho, r) = V_{conf}(r) e^{-c\rho r}\,, \tag{1.1}$$

where $r = |\boldsymbol{r}_1 - \boldsymbol{r}_2|$ is the relative interquark distance, $\rho = N/\Omega$ the (uniform) density of a system of N fermions in a volume Ω, c is a (dimensional) constant parameter and $V_{conf}(r)$ a suitably chosen confining potential. The string–flip model assumes the latter to be a linear or quadratic function of the distance: with the additional exponential factor, the potential (1.1) resembles a strong confining force only in the limit of very low densities (and for short distances), where pairs of quarks should be actually bound into hadrons, while it becomes negligible at large densities, where one expects the system to behave like a fermion gas (weakly interacting or even non–interacting "quark plasma").

In the present context the most interesting quantity, which allows to understand whether quarks are bound into pairs ("hadrons" in the present, colourless approach) or rather uniformly distributed as a non–interacting Fermi gas, is the so–called pair correlation function. It can be obtained from the expectation value of the two–body density operator:

$$g(r) = \frac{N(N-1)}{\rho^2} < \Psi | \rho_2(|\boldsymbol{r}_1 - \boldsymbol{r}_2|) | \Psi >, \tag{1.2}$$

where, for pointlike particles, the two–body density reads

$$\rho_2(|\boldsymbol{r}_1 - \boldsymbol{r}_2|) = \frac{1}{N(N-1)} \sum_{i \neq j} \delta(\boldsymbol{r}_i - \boldsymbol{r}_1) \delta(\boldsymbol{r}_j - \boldsymbol{r}_2), \tag{1.3}$$

and $|\Psi >$ is the exact (normalized) ground state of the system. For a system of strongly correlated pairs $g(r)$ will show up a well localized peak at small values of r, while the Fermi gas pair correlation function has a fairly constant behaviour, with the exception of small r values, where the Pauli principle prevents particles to be close to each other.

Another quantity which will be investigated here is the ground state energy of the system and its evolution with the density. In the current literature this is usually interpreted as the equation of state of the system, thus it can help in disentangling the occurrence of different "phases" in the evolution of the system.

The paper is organized as follows: in Sect. 2 we shortly present the formalism employed to find eigenvalues and eigenfunctions of the three-dimensional model. In Sect. 3 we discuss the numerical results, both for simple (harmonic or linear) confining potentials and for a more realistic Cornell potential. Finally in Sect. 4 we shortly discuss the implications of our calculation.

2 Three–dimensional system

The extension of the model of [10] to a three–dimensional system is straightforward. Nevertheless it is an important test, since the statistical properties of a one–dimensional system (and, specifically, the occurrence of phase transitions) sometimes depend on the considered dimensionality.

To start with, the quark–quark potential will be written as in (1.1), with a quadratic function for the confining force:

$$V^Q_{conf}(r) = \frac{1}{2} \alpha_q r^2\,. \tag{2.1}$$

In contrast with ref. [10] we shall consider here dimensional quantities, so that α_q has dimensions of energy $\times$ length^{-2}, and the constant c, in (1.1) acquires the dimensions of a length squared. Different density dependences (e.g. $\rho^{1/3}$, in order to leave a dimensionless c) have also been considered, with qualitatively similar results, but no compelling reason has been found to alter the original 1–Dim model.

We also take into account spin degrees of freedom, which enter into play in the definition of the symmetry properties of the two–quark states, although they are not relevant for the dynamical correlations, since in (2.1) no explicit spin dependence of the quark–quark interaction is assumed. Colour degrees of freedom are neglected as in the previous work.

Following the same procedure adopted to solve the 1–Dim problem, we obtain eigenfunctions and energy eigenvalues of the system, starting from the Schrödinger equation for the relative motion

$$H_{\rm rel} \psi_n(\boldsymbol{r}) = E_n \psi_n(\boldsymbol{r}) \tag{2.2}$$

where

$$H_{\rm rel} = -\frac{\hbar^2}{2\mu} \triangle + V(\rho, r)\,. \tag{2.3}$$

In the above $\mu = m_q/2$ is the reduced mass of the pair. We search for solutions of (2.2) corresponding to bound states by imposing the boundary condition[1]

$$\psi_n(\boldsymbol{r})|_{r=R} = 0 \tag{2.4}$$

for arbitrary values of R, beyond the "confining" region of the potential (1.1).

Due to the central nature of the latter it is convenient to work out the solution in spherical coordinates and set

$$\psi_n(\boldsymbol{r}) = \sum_{\ell=0}^{\infty} \sum_{m=-\ell}^{\ell} a^m_{n\ell} \varphi_{n\ell}(r) Y^m_\ell(\theta, \phi), \tag{2.5}$$

the Y^m_ℓ being the spherical harmonics (eigenfunctions of L^2 and L_z) and $\varphi_{n\ell}(r)$ the radial wavefunction which, in

[1] It should be noticed that the potential (1.1) with the confining force (2.1) does not admit, "stricto sensu", bound states, since $V(\rho, 0) = V(\rho, \infty) = 0$. However it displays a potential barrier which separates a confinement region around the origin from a free–motion regime at large distances. The transmission probability inversely depends upon the height of the barrier, and obviously increases with the density. With a different confining potential, like the Cornell one (see below), bound states are allowed even in the presence of the screening factor

turn, we express as a linear superposition of free solutions (the spherical Bessel functions):

$$\varphi_{n\ell}(r) = \sum_i \mathcal{N}_{i\ell} c^{\ell}_{ni} j_\ell(k_i r). \tag{2.6}$$

In solving the radial wave equation, the different partial waves are obviously decoupled from each other (and are degenerate with respect to m). Thus we can require that the condition (2.4) is separately satisfied by each partial wave $[\varphi_{n\ell}(R) = 0]$, the wavenumbers k_i being chosen within the discrete set of values (different for each ℓ–value) obeying[2]

$$j_\ell(k_i R) = 0\,. \tag{2.7}$$

With standard projection techniques one can transform the radial Schrödinger equation into the following algebraic system for the coefficients $b^m_{n\ell i} \equiv a^m_{n\ell} c^{\ell}_{ni}$:

$$\sum_i b^m_{n\ell i} \left[k_i^2 \delta_{ij} + \widetilde{\alpha} \mathcal{V}^{\ell}_{ij}\right] = b^m_{n\ell j} \mathcal{E}_n \tag{2.8}$$

where $\widetilde{\alpha} = (m_q/\hbar^2)\alpha_q$, $\mathcal{E}_n = (m_q/\hbar^2)E_n$ and

$$\mathcal{V}^{\ell}_{ij} = \mathcal{N}_{i\ell}\mathcal{N}_{j\ell} \frac{1}{\alpha} \int_0^R dr r^2 j_\ell(k_i r) j_\ell(k_j r) V(\rho, r), \tag{2.9}$$

the $\mathcal{N}_{i\ell}$ being the appropriate normalization constants

$$\mathcal{N}_{i\ell} = \sqrt{\frac{2}{R^3}} \frac{1}{|j_{\ell+1}(k_i R)|}, \tag{2.10}$$

which are required to normalize the spherical Bessel functions in a finite spherical volume of radius R:

$$\mathcal{N}_{i\ell}\mathcal{N}_{j\ell} \int_0^R dr r^2 j_\ell(k_i r) j_\ell(k_j r) = \delta_{ij} \quad (\forall \ell)\,. \tag{2.11}$$

The inclusion of spin degrees of freedom into the two–quark states amounts to consider, in $\psi_n(\boldsymbol{r})$, even partial waves associated with the (antisymmetric) singlet state $S = 0$, and odd partial waves together with the (symmetric) triplet states $S = 1$.

Moreover it is useful to define the following radial probability density:

$$\rho_n(r) = r^2 \int |\psi_n(\boldsymbol{r})|^2 d\Omega_r \equiv \sum_\ell \rho_{n\ell}(r), \tag{2.12}$$

where the partial wave contributions, derived from (2.5) and (2.6), read

$$\rho_{n\ell}(r) = r^2 \sum_{ij} {b^0_{n\ell i}}^* b^0_{n\ell j} \mathcal{N}_{i\ell}\mathcal{N}_{j\ell} \times (2\ell+1) j_\ell(k_i r) j_\ell(k_j r). \tag{2.13}$$

[We have assumed here, for simplicity, equal weight for the m–components, $b^m_{n\ell i} = b^0_{n\ell i}$, $(\forall m)$, which allows to perform the residual sum over m]. A few examples of $\rho_{n\ell}(r)$ are shown in Figs. 1 and 2. In the first figure the partial probability densities are evaluated at a rather low ($\rho = 0.1$ fm^{-3}) density, both for the ground ($n = 0$) and the first excited ($n = 1$) s–states; in this situation the potential (1.1) does not differ too much from the confining (quadratic) potential, at least for limited values of r: thus the partial probability densities turn out to be close to the corresponding quantities evaluated with a pure harmonic potential (dashed lines). In Fig. 2, instead, where only the ground state $\ell = 0$ partial density is shown, sizable deviations from the partial densities of the harmonic potential are already visible at $\rho = 0.3$ fm^{-3}, while for the even larger density $\rho = 0.5$ fm^{-3} the comparison of the partial probability density associated with the eigenfunctions of (1.1) is carried along with the one of a free Fermi gas (dot–dashed line): the similarity between the two shows that at this density the interquark potential is already rather weak.

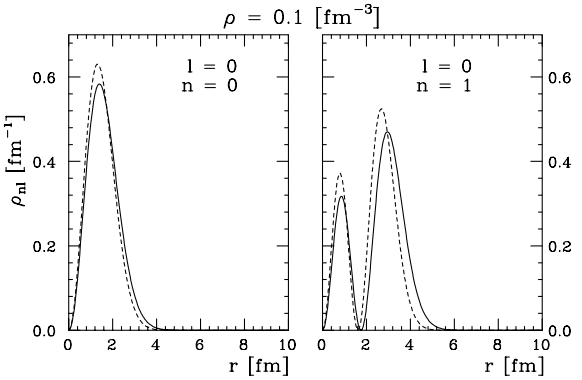

Fig. 1. Partial wave ($\ell = 0$) contribution to the radial probability density $\rho_{00}(r)$ (left) and $\rho_{10}(r)$ (right) obtained from the eigenfunctions of the potential (1.1) with $V^Q_{conf} = \alpha_q r^2/2$ (continuous lines). The corresponding quantities for the pure V^Q_{conf} are also shown (dashed lines). The density is $\rho = 0.1$ fm^{-3}

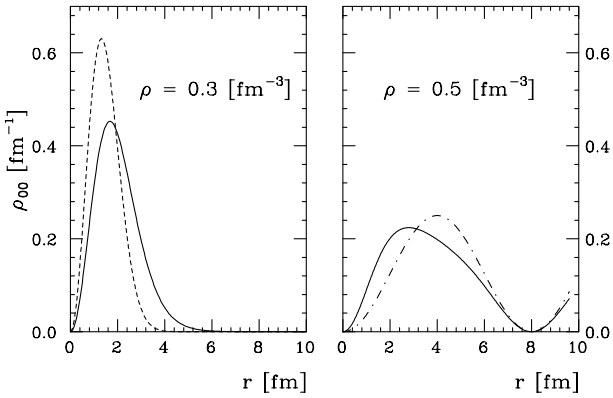

Fig. 2. Partial wave ($\ell = 0$) contribution to the radial probability density $\rho_{00}(r)$ at $\rho = 0.3$ fm^{-3} (left) and $\rho = 0.5$ fm^{-3} (right): the $\rho_{00}(r)$ obtained from the eigenfunctions of the potential (1.1) (continuous line in both figures) is compared with the corresponding quantity for the pure V^Q_{conf} (left, dashed line) and with the partial probability density for a free Fermi gas (right, dot dashed line)

[2] In this work, typical values of R are in the range $8 \div 10$ fm

The same technique utilized for solving the Schrödinger equation can now be applied to obtain the solution of the corresponding Bethe–Goldstone (BG) equation; in this case the two–body wavefunction for the relative motion must incorporate the Pauli correlations induced by the medium. The formal expansion (2.6) must then be modified within the independent pair approximation, assuming that all single particle states with momentum $k_i \leq k_F$ are occupied as in the ground state of the free Fermi gas (we remind that for a three–dimensional Fermi gas the relationship between the density and the Fermi momentum is: $\rho = k_F^3/3\pi^2$). This obviously sets a constraint on the available momenta for the relative motion of a correlated pair. Indeed by defining

$$\boldsymbol{k} = \frac{\boldsymbol{k}_1 - \boldsymbol{k}_2}{2}, \qquad \boldsymbol{K} = \boldsymbol{k}_1 + \boldsymbol{k}_2\,, \tag{2.14}$$

the series (2.6) will include now, beyond an "unperturbed" term proportional to $j_\ell(kr)$, which fixes the relative momentum k of the pair (with $\boldsymbol{k}_1, \boldsymbol{k}_2$ inside the Fermi sphere), only terms with $\boldsymbol{k}_a \equiv (\boldsymbol{k}_1' - \boldsymbol{k}_2')/2$ satisfying the condition $k_1', k_2' > k_F$:

$$\chi_{n\ell,kK}(r) = \mathcal{N}_{0\ell} c^\ell_{n0} j_\ell(kr) + \sum_a \mathcal{Q}(\boldsymbol{K}, \boldsymbol{k}_a) \mathcal{N}_{a\ell} c^\ell_{na} j_\ell(k_a r)\,. \tag{2.15}$$

In the above equation we have introduced the Pauli operator

$$\mathcal{Q}(\boldsymbol{K}, \boldsymbol{k}_a) = \theta\left(\left|\frac{\boldsymbol{K}}{2} + \boldsymbol{k}_a\right| - k_F\right) \times \theta\left(\left|\frac{\boldsymbol{K}}{2} - \boldsymbol{k}_a\right| - k_F\right) \tag{2.16}$$

which obviously depends on both the relative and the total momentum of the pair of particles, the latter being conserved in all terms of the expansion (2.15). Here have adopted the customary [12] angle averaged Pauli operator, $\mathcal{Q}(K, k_a) \equiv \langle \mathcal{Q}(\boldsymbol{K}, \boldsymbol{k}_a) \rangle$. Thus we can obtain the coefficients c^ℓ_{na}, for each partial wave ℓ of the correlated wave function (2.15), by solving the algebraic system:

$$\left(\mathcal{E}^{BG}_n - k_b^2\right) c^\ell_{nb} \mathcal{Q}(K, k_b) - \widetilde{\alpha} \sum_a \mathcal{V}^\ell_{ab} c^\ell_{na} \mathcal{Q}(K, k_a) = 0, \tag{2.17}$$

The Bethe–Goldstone wavefunction for a pair of particles will then read

$$\begin{aligned} \Psi_{\boldsymbol{K},\boldsymbol{k}}(\boldsymbol{R}, \boldsymbol{r}) &= \Phi^{CM}_{\boldsymbol{K}}(\boldsymbol{R}) \psi^{BG}_{n,\boldsymbol{kK}}(\boldsymbol{r}) \\ &= \Phi^{CM}_{\boldsymbol{K}}(\boldsymbol{R}) \sum_{\ell m} a^m_{n\ell} \chi_{n\ell,kK}(r) Y^m_l(\Omega_r) \end{aligned} \tag{2.18}$$

the CM wave function being a plane wave. The radial probability density (2.12) can be defined also for the Bethe–Goldstone solutions, but now this quantity will depend upon k and K: although the dependence on these quantum numbers turns out to be mild, it will be more convenient to consider, instead, the two–body correlation function.

In what follows we have taken into account only the first two partial waves ($\ell = 0, 1$) since our main interest is focussed on the existence of the *bound states* of a pair and on their evolution with the density: for higher angular momentum eigenvalues the centrifugal force largely overcomes the binding effects of the two–body interaction potential and the corresponding states belong to the continuum.

2.1 The equation of state

In solving the Bethe–Goldstone equation, one gets both eigenfunctions and eigenvalues of the relative motion; we can thus consider the ground state energy (per particle) of the system, which, in the thermodynamical limit of a very large system ($N, \Omega \to \infty$, with fixed $\rho = N/\Omega$), can be written as follows:

$$\begin{aligned} \varepsilon \equiv \frac{E}{N} &= \frac{1}{2\rho^2} \sum_{S,M_S} \int \frac{d^3k}{(2\pi)^3} \int \frac{d^3K}{(2\pi)^3} \\ &\quad \times \theta\left(k_F - |\boldsymbol{K}/2 + \boldsymbol{k}|\right) \theta\left(k_F - |\boldsymbol{K}/2 - \boldsymbol{k}|\right) E^{(S)}_{\boldsymbol{kK}} \\ &= \frac{1}{8\rho^2\pi^4} \int_0^\infty k^2 dk \\ &\quad \times \int_0^\infty dK\, K^2\, \mathcal{I}(k, K) \left(E^{(0)}_{\boldsymbol{kK}} + 3E^{(1)}_{\boldsymbol{kK}}\right)\,. \end{aligned} \tag{2.19}$$

In the above $S(M_S)$ denote the spin quantum numbers: we remind that, to preserve antisymmetrization, the singlet state $S = 0$ is uniquely associated with even spatial wave functions (here $\ell = 0$), while the triplet $S = 1$ states are associated with odd spatial wave functions ($\ell = 1$). Moreover $E_{\boldsymbol{kK}} = E_{CM} + E^{BG}_{\boldsymbol{kK}}$, with $E_{CM} = \hbar^2 \boldsymbol{K}^2/4m_q$ and $\mathcal{I}(k, K)$ is the result of the (analytical) integration over the angle between $\boldsymbol{k}$ and $\boldsymbol{K}$. The latter appears only in the θ–functions of the r.h.s. of (2.19) since, using the Pauli averaged operator, the BG solutions are independent on the direction of $\boldsymbol{K}$.

It is interesting to compare the above evaluation of the energy per particle, which includes *both* the dynamical and the statistical (Pauli) correlations, with the Hartree–Fock (HF) approximation,

$$\begin{aligned} \varepsilon_{HF} &= \frac{3}{5}\varepsilon_F + U_{HF} \\ &= \frac{3}{5}\varepsilon_F + \frac{1}{8\rho^2\pi^4} \int_0^\infty k^2 dk \\ &\quad \times \int_0^\infty dK K^2 \mathcal{I}(k, K) \left[V_0(k) + 3V_1(k)\right]\,, \end{aligned} \tag{2.20}$$

ε_F being the free Fermi energy and:

$$V_\ell(k) = \int_0^R dr r^2 \left\{\mathcal{N}_{k\ell} j_\ell(kr)\right\}^2 V(\rho, r)\,. \tag{2.21}$$

Obviously the HF scheme accounts for the interaction only through an average, one–body mean field, thus describing, in principle, a system of independent particles.

We will show in the next section that the HF approximation fails in describing the system at low densities, where the HF energy per particle diverges. Instead a proper treatment of two–body correlations provides finite, sensible results.

2.2 The pair correlation function

The two–body correlation function defined in (1.2) can be evaluated using the Bethe–Goldstone ground state wave function:

$$g(r) = \frac{N(N-1)}{\rho^2} < \Psi^{BG}|\rho_2(|\boldsymbol{r}_1 - \boldsymbol{r}_2|)|\Psi^{BG} > = \frac{1}{\rho^2}\int \frac{d^3k}{(2\pi)^3} \times \int \frac{d^3K}{(2\pi)^3}\theta\left(k_F - |\boldsymbol{K}/2 + \boldsymbol{k}|\right)\theta\left(k_F - |\boldsymbol{K}/2 - \boldsymbol{k}|\right) \times \left\{|\psi_{n0,\boldsymbol{kK}}(\boldsymbol{r})|^2 + 3\,|\psi_{n1,\boldsymbol{kK}}(\boldsymbol{r})|^2\right\} \quad (2.22)$$

In deriving (2.22) we have obviously used the same set of states which were employed for the evaluation of the ground state energy of the system. Again the angular integrations in (2.22) can be analytically performed, as in (2.19), since the BG wave functions do not depend on the direction of $\boldsymbol{K}$.

To appreciate the amount of correlations (both dynamical and statistical) embodied by $g(r)$ it is useful to compare it with the corresponding quantity evaluated in a Fermi gas:

$$g_{FG}(r) = \frac{1}{\rho^2}\int \frac{d^3k}{(2\pi)^3} \times \int \frac{d^3K}{(2\pi)^3}\theta\left(k_F - |\boldsymbol{K}/2 + \boldsymbol{k}|\right)\theta\left(k_F - |\boldsymbol{K}/2 - \boldsymbol{k}|\right) \left\{[\mathcal{N}_{k0} j_0(kr)]^2 + 3\,[\mathcal{N}_{k1} j_1(kr)]^2\right\} \quad (2.23)$$

where the radial correlated wave functions are replaced by the spherical Bessel functions, with the appropriate normalization.

3 Results

For an explicit evaluation of (2.19) and (2.22) we have to specify our choice of the model parameters: for the quark mass (in the kinetic term of the Hamiltonian) we use the reference value $m_q = 220$ MeV/c, which has been employed in various non–relativistic quark models to fit hadron spectroscopy (see, for example, [8]); the strength α_q of the harmonic potential, (2.1), has been fixed to the value $\alpha_q = 120$ MeV fm^{-2}, in order to have hadronic dimensions of the order of about 1 fm, though we have not attempted a precise fit. Finally we have to choose the c parameter in the exponent of (1.1): clearly its value affects the density dependence of the interaction and, for the sake of illustration, we shall adopt two typical and rather extreme values: $c = 1$ fm^2 and $c = 0.1$ fm^2.

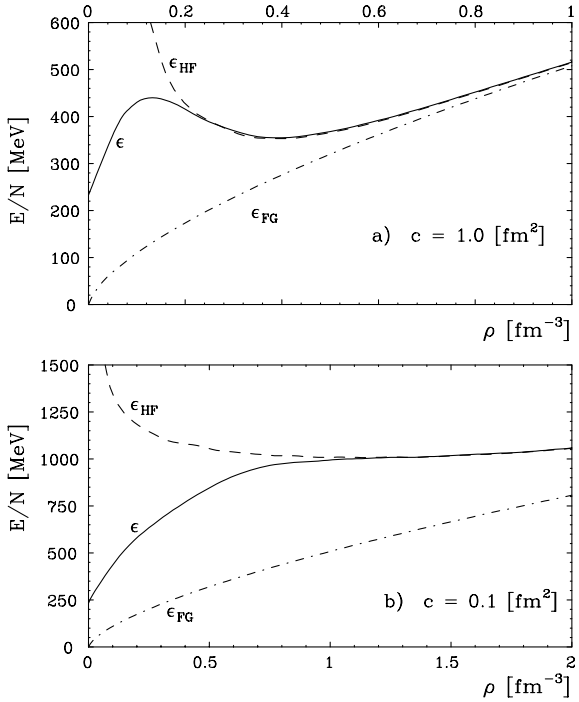

Fig. 3. Ground state energy per particle, (2.19) versus the density ρ (continuous line), compared with the HF energy per particle (dashed line) and to the pure kinetic energy of a Fermi gas (dot–dashed line). The quadratic confining potential (2.1) is employed. In **a** the c value is ten times bigger that in **b**

The correlated and HF energy per particle for the quadratic confining potential are shown in Fig. 3a ($c = 1$ fm^2) and 3b ($c = 0.1$ fm^2), together with the average kinetic energy of a free Fermi gas (ε_F), as a function of the density: in both cases there exists a "critical density", ρ_c, at which the correlated and mean–field (HF) energies coincide: this fact implies that the medium correlations taken into account by the Bethe–Goldstone equation no longer affect the relative motion of a pair and for $\rho > \rho_c$ the system can be regarded as a gas of independent quarks, whose (weak) interaction is embodied in the mean Hartree–Fock field, gradually vanishing with increasing density.

Although, in the present treatment, we cannot identify a specific order parameter, which would allow to consider the phase transition from a thermodynamical point of view, we have interpreted as a transition density, ρ_c, the one where the *medium induced* correlations vanish: this quantity can be defined as the average value (with respect to the relative and total momentum of a pair) of the difference between the matrix elements of the bare potential (1.1) and the G-matrix which one obtains from the solution of the Bethe–Goldstone equation:

$$\Delta U(\rho) = \overline{< \boldsymbol{k}, \boldsymbol{K}|V|\boldsymbol{k}, \boldsymbol{K} >} - \overline{< \boldsymbol{k}, \boldsymbol{K}|G|\boldsymbol{k}, \boldsymbol{K} >}. \quad (3.1)$$

The choice of ΔU as an "order parameter" is arbitrary, but it is closely related to the energy gap usually considered in

the microscopic description of superconductivity; in that case a non–vanishing gap signals the existence of bound electron pairs which profoundly alter the global properties of the system. Here we assume (3.1) as a discriminant between a system of "hadrons" (bound pairs of quarks) and a weakly interacting Fermi gas of quarks.

One can see in Fig. 3 that not only the value of the above defined critical density depends (as it is rather obvious) upon c, being $\rho_c \simeq 0.2$ fm^{-3} for $c = 1$ fm^2 and $\rho_c \simeq 1$ fm^{-3} for $c = 0.1$ fm^2, but also the behaviour of $\varepsilon(\rho)$ with the density is different in the two cases: this implies that the energy of a correlated pair does not simply scale as the bare interaction (1.1), which depends on the product $c\rho$ alone. Indeed the loss of the scaling property must be ascribed to the density dependence of the Pauli correlations in the Bethe–Goldstone equation from which $\varepsilon(\rho)$ is obtained. In other words, while the Hamiltonian is scale invariant, the BG solution is not.

We notice that the transition from the zero density limit [$\varepsilon(\rho = 0) \simeq 230$ MeV] to the high density regime of independent particles is quite smooth and monotonic for $c = 0.1$ fm^2, but goes instead through a maximum for $c = 1$ fm^2, which better suites, at least qualitatively, to the hypothesis of a phase transition between two "stable" regimes. It might be worth reminding that the behaviour illustrated in Fig. 3a closely resembles the analogous result of [5].

It is also interesting to compare the above discussed equation of state with the one obtained, within the same theoretical framework, using a somewhat different confining potential, namely

$$V^L_{conf}(r) = \frac{1}{2}\alpha_l r\,. \tag{3.2}$$

We have assumed $\alpha_l = 445$ MeV fm^{-1} and $c = 0.5$ fm^2 (in the density dependent exponential of the full potential), in such a way that at $\rho = 0.2$ fm^{-3} the potentials $V(\rho, r)$ stemming from the quadratic and from the linear confining interactions display a fairly similar behaviour. One should remind that a linear quark–quark potential can be motivated on the basis of lattice QCD calculations, and is employed in many phenomenological constituent quark models (e.g. [8,9]).

The energy per particle obtained with the potential (3.2) is displayed in Fig. 4, which is qualitatively similar to Fig. 3a, although the maximum in the BG correlated energy seems to be less pronounced than in the case of the harmonic potential, and the critical density is somewhat higher ($\rho_c \simeq 0.3$ fm^{-3}). Hence, independently on the specific form of the confining potential, the main features of the equation of state for the correlated system remain fairly unchanged, providing we keep the same density dependence of the two–body interaction.

It is worth to notice, at this point, that the total energy per particle rapidly exceedes, with increasing density, the rest mass of the quark, thus posing serious doubts on the validity of the non–relativistic treatment adopted here. Of this effect it is largely responsible the average kinetic energy, which grows as $\rho^{2/3}$ and which becomes dominant

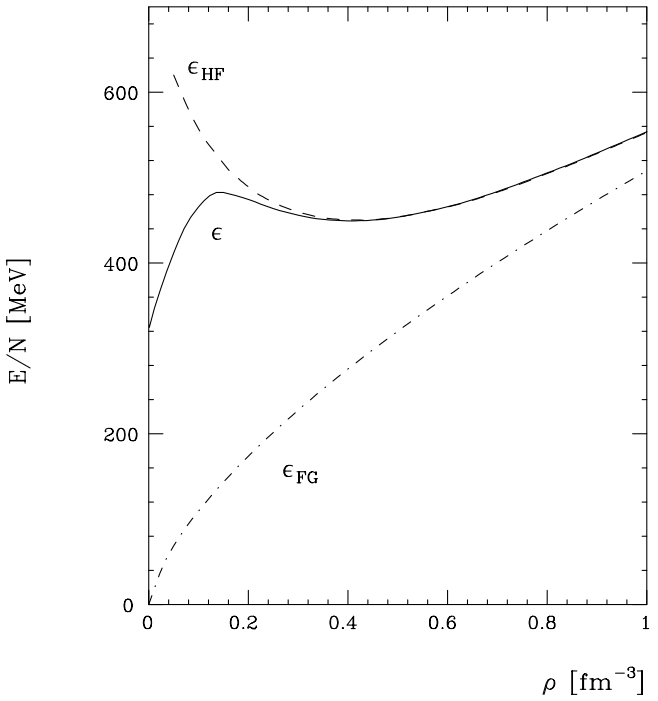

Fig. 4. The same as Fig. 3a, but utilizing the linear confining potential (3.2), with the parameters given in the text

above the critical density; as a consequence of the density dependence of the interaction, asymptotically the system behaves as a free Fermi gas and could be dealt with relativistically, thus avoiding the risk of getting an acausal equation of state. However a relativistic approach is not so obvious in the presence of the interaction: thus in the next subsection we shall limit ourselves to give an approximate but quantitative estimate of the effects associated with a relativistic kinematics.

Turning to the pair correlation function (2.22), it is illustrated in Fig. 5 for the quadratic confining potential (2.1), at $\rho = 0.2$ fm^{-3} with $c = 1$ fm^2 and $\alpha_q = 120$ MeV fm^{-2}. Together with the full result for the correlation function obtained from the solution of the BG equation (continuous line), the separate $\ell = 0$ (dashed line) and $\ell = 1$ (dot–dashed line) contributions are displayed: the latter obviously moves the average separation distance toward bigger values. The comparison with the free Fermi gas result (dotted line) shows that at this density the system is approaching the transition point, as it was argued from the energy per particle of Fig. 3a (obtained with the same c value): indeed the Fermi gas component at large distances is already quite important in the correlated $g(r)$. Still, however, the latter displays a large probability for a bound pair with a size of the order of $r = 1.9 \div 2$ fm.

The evolution of the BG pair correlation function with the density is shown in Fig. 6, where $g(r)$ is displayed for densities ranging from 0.1 to 0.5 fm^{-3}. The presence of a bound state is clearly manifest at $\rho = 0.1$ fm^{-3}, while, with increasing density, the Fermi gas component develops at large distances, and at $\rho = 0.5$ fm^{-3} the correlation

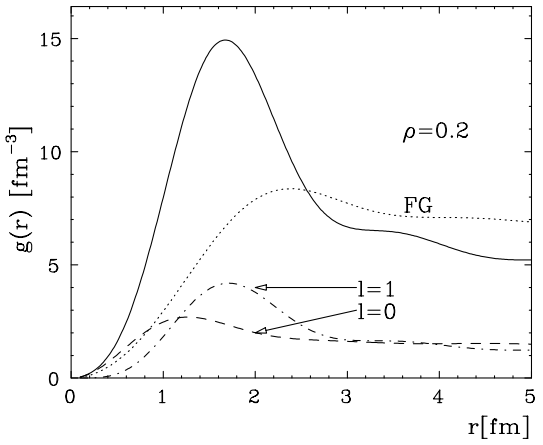

Fig. 5. The pair correlation function $g(r)$ derived, with the quadratic potential (2.1), from the Bethe–Goldstone wave functions is displayed as a function of the relative interquark distance (continuous line): the density is fixed to the value $\rho = 0.2$ fm^{-3}. The separate $\ell = 0$ (dashed line) and $\ell = 1$ (dot–dashed line) contributions are also shown. The dotted curve corresponds to the free Fermi gas correlation function, at the chosen density

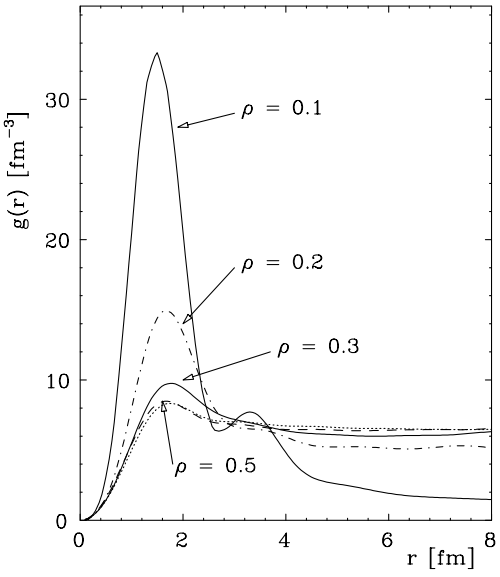

Fig. 6. The pair correlation function $g(r)$ derived from the Bethe–Goldstone wave functions is displayed as a function of the relative interquark distance at various densities: $\rho = 0.1$ fm^{-3} (thick solid line), $\rho = 0.2$ fm^{-3} (dot–dashed line), $\rho = 0.3$ fm^{-3} (thin solid line) and $\rho = 0.5$ fm^{-3} (dashed line). For the last density value the Fermi gas correlation function is also shown (dotted line). The BG solutions refer to the quadratic confining potential (2.1)

function for the interacting system (dashed line) can be hardly distinguished from the one of the Fermi gas, represented by the dotted line. Similar results are obtained with the linear confining potential of (3.2).

3.1 Application to the Cornell potential

Many static potentials, sometimes "motivated" from QCD, have been proposed in the past in the attempt to reproduce mesonic and baryonic spectra in terms of bound states of quarks. The full complexity of hadron spectroscopy requires indeed complicated functional forms, with spin and colour dependent terms (see, e.g., [8,9]). We have chosen here the Cornell potential [13], which is one of the earliest QCD motivated quark–quark potential but, in spite of its relative simplicity, it has been fairly successfully employed to fit heavy quarkonia [14,15]. It has the form:

$$V_{Cornell}(r) = -\frac{a}{r} + br + K\,, \tag{3.3}$$

where a, b and K are constants. It contains the typical Coulomb–like term, which can be motivated, at small r, by lowest order perturbative QCD, where a term α_s/r should account both for the perturbative one–gluon exchange and, in a string picture, for the transverse vibrations of the string. At large r perturbation theory breaks down and the linear term is essentially justified by lattice calculations.

We have then multiplied (3.3) by the usual density dependent factor:

$$V(r,\rho) = V_{Cornell}(r)e^{-c\rho r} \tag{3.4}$$

and we have employed this potential within the same theoretical framework illustrated in the previous section.

It is interesting to note that in [17] an analogous exponential screening factor has been adopted, in connection with the Cornell potential, to account for the deconfinement of heavy quarks bound states at finite temperature: in the above mentioned paper the temperature dependent chemical potential plays the role which we ascribe to the density of the system and it is found that with increasing $\mu(T)$ the dissociation energy of a heavy $q\bar{q}$ pair rapidly vanishes.

Here we have utilized the Cornell potential with the following (standard) values of the parameters: $a = 92.73$ MeV fm, $b = 942.7$ MeV fm^{-1}, $K = -802$ MeV. The latter have been used in [15] together with rather large quark masses, typically to explore the heavy quarkonia: we shall adopt here the same light constituent quark mass utilized above ($m_q = 220$ MeV) together with the value $c = 1.5$ fm^2.

In solving the Bethe–Goldstone equation for the relative motion of a pair, one should notice that the Coulomb–like term of the Cornell potential requires a careful numerical treatment in the matrix elements of the potential between unperturbed states [see (2.9)].

We display in Fig. 7 the equation of state (continuous line labelled ϵ) obtained with the screened Cornell potential: it closely resembles the results previously obtained with the more schematic quadratic (with $c = 1$ fm^2) or linear potentials. The critical density, where the correlated energy coincides with the HF one, is about 0.5 fm^{-3}. Also in this case, as in the previous Figs. 3 and 4, the energy

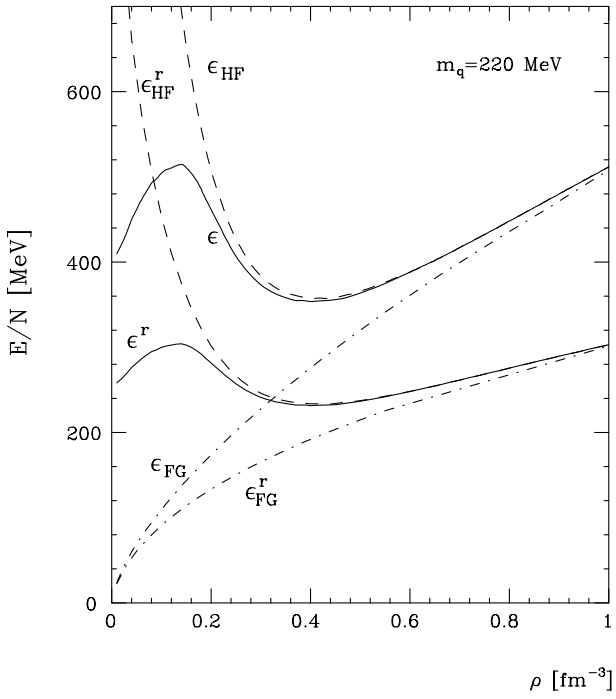

Fig. 7. Ground state energy per particle, (2.19) versus the density ρ (continuous line), compared with the HF energy per particle (dashed line) and to the pure kinetic energy of a Fermi gas (dot–dashed line). The screened Cornell potential (3.4) is employed, for quarks of mass $m_q = 220$ MeV. Also shown (using, correspondingly, the same symbols) are the "relativistic" estimates of the same quantities as obtained from (3.5); the latter are labelled by symbols with a superscript "r"

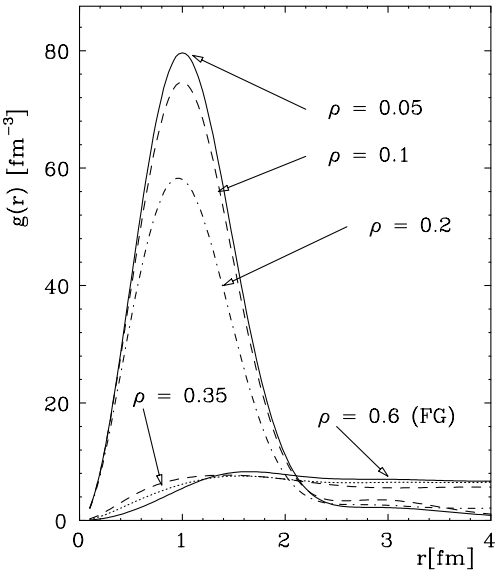

Fig. 8. The pair correlation function $g(r)$ derived from the Bethe–Goldstone wave functions for the Cornell potential (3.4) and $m_q = 220$ MeV is displayed as a function of the relative interquark distance at various densities: $\rho = 0.05$ fm^{-3} (thick solid line), $\rho = 0.1$ fm^{-3} (dashed line), $\rho = 0.2$ fm^{-3} (dot–dashed line), $\rho = 0.35$ fm^{-3} (dashed line) and $\rho = 0.6$ fm^{-3} (dotted line). For the last density value the Fermi gas correlation function is also shown (thin solid line)

per particle rapidly reaches, with increasing density, more than twice the value of the rest mass of the quark, hence hindering the non–relativistic approach. In order to get a rough estimate of what the corresponding relativistic equation of state would look like, we have adopted a simple prescription, already utilized in [15]; it amounts to replace the non–relativistic energy eigenvalues ϵ by:

$$\epsilon^r = \sqrt{m_q^2 + 2m_q\epsilon} - m_q \,. \tag{3.5}$$

The correlated energy per particle obtained from (3.5) is shown in Fig.7 by the continuous line labelled ϵ^r and clearly appears more sound with respect to the value of the quark rest mass. We also display the results of (3.5) for the Hartree–Fock (ϵ^r_{HF}) and the free Fermi Gas (ϵ^r_{FG}) energies. It is important to notice that this procedure does not alter the value of the transition density. Thus our conclusions on the evolution of the system with the density is not essentially altered. Obviously we cannot claim that these results take into account properly the relativistic nature of the system: yet at large densities, where the pure kinetic energy survives, our approximation should be sound, while at low densities, up to the occurrence of the transition investigated here, we can expect the non–relativistic result to be correct.

The analysis of the pair correlation function obtained with the Cornell potential leads to analogous considerations: in Fig. 8 we show a few examples of $g(r)$ at different values of the density. The free Fermi gas two–body correlation function is recovered for $\rho \simeq 0.6$ fm^{-3}, in agreement with the results obtained in the equation of state.

4 Conclusions

In this work we have considered a system of fermions interacting through a density–dependent potential: the main purpose was to show that, as the density increases, the system evolves from an assembly of bound pairs to a non–interacting Fermi gas. This outcome is obviously related to the exponential screening (proportional to the density) in the potential (1.1): however we show that the occurrence of a sort of deconfinement phase transition is non–trivially linked to the effect of the medium: indeed the latter intervenes not only through the density dependence of the two–body interaction, but also through the Pauli correlations, whose relevance increases with the density of the medium.

Indeed a central point in the present calculations is the interplay between the increasing Pauli–blocking effect on the Bethe–Goldstone wavefunction and the decreasing efficacy of the interquark potential in producing a stable binding of the pairs.

Another interesting outcome of the present work is the similarity of the results for the three–dimensional system to the ones obtained for a single spatial dimension [10]: in going from one to three spatial dimensions, the critical

behaviour of the system does not seem to be substantially affected.

At variance with the one–dimensional case, we have employed here different forms for the confining potential: in addition to the quadratic potential of [10], we have also considered a linear one and a the more realistic Cornell potential. In all instances the low density confined phase gradually evolves into a regime in which medium effects and dynamical correlations are negligible, the fermions being deconfined. This behaviour turns out to be fairly independent upon the specific confining potential.

Of course the density dependence of the interaction adopted here has no microscopic foundation; but a similar screening of the color interaction, induced by a finite temperature of the many–body system, was obtained in the past by summing an infinite chain of one–loop insertions in the gluon propagator [16] and, more recently, utilized in the investigation of the deconfinement of heavy vector mesons [17].

From the above results we can conclude that the deconfinement phase transition occurs in a many fermion system under the following conditions: i) the attractive two–body interaction, which produces two or more quark bound states, is screened in the presence of a *dense* medium; ii) the action of the medium is accounted for not only in the two–body dynamics (through the above mentioned, phenomenological, screening mechanism) but also from the statistical point of view, through the effect of the Pauli principle, which strongly modifies the quark–quark interaction.

This work was supported in part by the European Network ERB CH RX-CT 93-0323 and by grant KBN/IFJ/046/1995.

References

1. C. Lourenço, Proceedings of *Quark matter '96*, Nucl. Phys. **A 610**, 552c (1996)
2. T. Matsui and H. Satz, Phys. Lett. **178B**, 416 (1986)
3. D. Kharzeev, C. Lourenço, M. Nardi and H. Satz, Z.Phys. **C74**, 307 (1997); D. Kharzeev, M. Nardi and H. Satz, Preprint hep-ph/9707308
4. C.J. Horowitz, E.J. Moniz and J.W. Negele, Phys. Rev. **D 31**, 1689 (1985)
5. C.J. Horowitz and J. Piekarewicz, Nucl. Phys. **A 536**, 669 (1992)
6. C.J. Horowitz and J. Piekarewicz, Phys. Rev. **C 44**, 2753 (1991)
7. W.M. Alberico, M.B. Barbaro, A. Molinari and F. Palumbo, Z. Phys. **A 341**, 327 (1992)
8. S.Godfrey and N.Isgur, Phys. Rev. **D 32**, 189 (1985)
9. S. Capstick and N. Isgur, Phys. Rev. **D 34**, 2809 (1986)
10. W.M. Alberico, M.B. Barbaro, A. Magni and M. Nardi, Nucl. Phys. **A 552**, 495 (1993)
11. W.M. Alberico, M. Nardi and S. Quattroccolo, Nucl. Phys. **A 589**, 620 (1995)
12. H.A. Bethe, Ann. Rev. of Nucl. Sci., vol. **21** (1971)
13. E. Eichten *et al.*, Phys. Rev. **D 17**, 3090 (1978); Phys. Rev. **D 21**, 203 (1980)
14. D.B. Lichtenberg, E. Predazzi, R. Roncaglia, M. Rosso and J.G. Wills, Z. Phys. C **41**, 615 (1989)
15. D.B. Lichtenberg, E. Predazzi, R. Roncaglia, M. Rosso and J.G. Wills, Z. Phys. C **46**, 75 (1990)
16. J. Kapusta, Nucl. Phys. **B 148** (1979), 461
17. F. Karsch, M.T. Mehr and H. Satz, Z. Phys. C **37**, 617 (1988)